Min, R.; Pereira, L.; Paixao, T.; Woyessa, G.; Hu, X.; Antunes, P.; André, P.... (2021). Chirped POF Bragg grating production utilizing UV cure adhesive coating for multiparameter sensing. Optical Fiber Technology. 65:1-7. https://doi.org/10.1016/j.yofte.2021.102593

Chirped POF Bragg grating production utilizing UV cure adhesive coating for multiparameter sensing

Rui Min,[1,*] Luis Pereira,[2] Tiago Paixao,[2] Getinet Woyessa,[3] Xuehao Hu,[4] Paulo Antunes,[2] Paulo Andre,[5] Ole Bang,[3,6] Joao Pinto,[2] Beatriz Ortega,[7] and Carlos Marques[2]

[1] Center for Cognition and Neuroergonomics, State Key Laboratory of Cognitive Neuroscience and Learning, Beijing Normal University at Zhuhai, 519087 Zhuhai, China

[2] I3N & Physics Department, Universidade de Aveiro, 3810-193 Aveiro, Portugal

[3] DTU Fotonik, Department of Photonics Engineering, Technical University of Denmark, Denmark

[4] Research Center for Advanced Optics and Photoelectronics, Department of Physics, College of Science, Shantou University, 515063 Guangdong, China

[5]Department of Electrical and Computer Engineering and Instituto de Telecomunicações, Instituto Superior Técnico, Universidade de Lisboa, 1049-001 Lisbon,Portugal

[6] SHUTE Sensing Solutions A/S, Oldenvej 1A, 3490 Kvistgård, Denmark

[7] ITEAM Research Institute, Universitat Politècnica de València, 46022 Valencia, Spain

** email: rumi@doctor.upv.es*

Abstract: In this work, we obtained chirped Bragg gratings by post-coating uniform poly (methylmethacrylate) (PMMA) microstructured polymer optical fiber Bragg gratings (POFBGs) with an UV cure adhesive. The main advantage of the proposed method consists on being a cost-effective and simple solution, since no special phase mask, additional etching or gradient thermal annealing are required. A comparison between the fabricated chirped Bragg grating's performance and previous reported methods in the literature is presented. As a compact sensor with two different active areas (adhesive coated and uncoated sections of the POFBG), the developed sensing device can be used for multiparameter sensing, namely for strain, humidity and temperature monitoring. Allying the proposed flexible and low-cost fabrication technique with the intrinsic characteristics of POFs, one may conclude that the developed sensor has high potential for multiparameter sensing in possible future engineering and biomedical applications.

Keywords: Polymer optical fiber, Fiber Bragg grating, Laser irradiation, Fiber sensing

1. Introduction

During the last decades, optical fiber sensors have been widely used to detect physical and chemical

parameters due to their advantages, such as the immunity to electromagnetic fields, small size and the ability to multiplex signals, among others [1]. Fiber Bragg grating (FBG) technology is one of the main solutions for fiber sensing, being extensively studied in silica fibers for more than thirty years [1]. In polymer optical fibers (POFs), FBG devices are also attractive for a wide range of sensing applications due to the intrinsic properties of these fibers, such as the lower Young's modulus, larger elongation capability and higher thermo-optic coefficient [2]. Furthermore, POFs are also suitable for biosensing applications [3-5], due to the non-brittle nature, higher bending flexibility and biocompatibility. Since the first polymer optical fiber Bragg grating (POFBG), which was reported in 1999 by *Peng et al*, using poly (methylmethacrylate) (PMMA) step-index POF [6], different polymer materials have been used for POFBG fabrication with specific purposes, such as high temperature resistance and humidity insensitive polycarbonate [7-8], Zeonex [9-10], Topas [11-12] and low attenuation CYTOP [13-14]. Using and mixing different polymers can also provide additional advantages, such as simultaneous humidity and temperature sensing, as demonstrated in a POF with Zeonex core and PMMA cladding [15]. Nonetheless, PMMA is the most common material for Bragg grating devices fabrication in POFs, due to the easy handling and processing, low cost and the relative easier grating inscription process with ultraviolet (UV) laser systems [16].

Similar to the FBGs, special grating devices are attractive for a variety of applications, and their production in POF allows to combine their optical performance with the POF physical properties. Some relevant examples are the phase shifted (PS) FBGs, which have been recently demonstrated as promising for ultrasonic detection [17], and tilted FBGs, which were firstly reported by *Hu et al.,* in 2014 [18], and have been also implemented for surface plasmon detection [19]. Chirped FBGs (CFBG) are attractive for applications such as dispersion compensation in long haul optical communication link [20], thermal profile detection in biomedical area [21], and ultra-sensitive liquid level indicator [22]. More specifically, some biomedical applications require to combine some sensing features, such as temperature and pressure, into an individual multi-parametric compact probe, in order to expand the measurement capacity over a short

length. Although CFBGs in POF were first proposed in 2005, for tunable dispersion with fixed wavelength [23], the first CFBG inscribed in POF was obtained in 2017, by using a 25 mm long chirped phase mask customized for 1550 nm wavelength [24]. Despite the chirped phase mask method offering high stability and repeatability, this technique presents several drawbacks, such as high-cost and lack of flexibility [24]. In the last years, several techniques have been proposed for fabricating chirped gratings in POF. *Theodosiou et al.* employed the femtosecond laser direct writing method in commercial CYTOP POF in 2018 [25], to fabricate a CFBG consisting of 2000 periods with a total length of ~ 4.5 mm and 10 nm bandwidth. *Min et al.* fabricated the first tunable chirped FBG in a tapered *benzil dimethyl ketal* (BDK) doped mPOF, by using a uniform phase mask under 248 nm radiation [26]. A chirp of ~0.26 nm/mm under 1.6% strain was obtained in a 10 mm long grating, and the tunable properties were given by the strain and temperature sensitivities of 0.71 ± 0.02 pm/με and 56.7 pm/ºC, respectively. *Min et al.* also fabricated chirped POFBGs by hot water assisted gradient thermal annealing of uniform POFBGs, showing up to 11 nm bandwidth over a 10 mm long grating at 850 nm region [27]. This method enabled the tuning of the wavelength and the chirp characteristics by accurate gradient thermal annealing. However, this method is based on partially pre-annealed POF, which consists on a major drawback since long stability is limited.

Therefore, the development of CFBGs by employing new techniques becomes important in order to simplify their production and mitigate the major drawbacks of the existing methods. For instance, the proper use of coatings assisted by strain appliance can be seen as a viable solution to develop CFBGs in already produced uniform FBGs. Among coating solutions, UV-curing optical adhesives, which are a clear, solvent-free material designed to be fully cured in a few minutes by ultraviolet (UV) light exposure, appears as a feasible solution. Normally, it is used for butt coupling between POFs and silica fibers, and to fabricate Fabry–Pérot cavities between two fiber end faces for sensing and filtering applications. *Hu et al.* reported on the employment of optical adhesive for butt coupling between silica pigtail and POF, using a UV cure adhesive (NOA 78, from Norland) with a modulus of elasticity of 1140 psi and a tensile strength of 649 psi*)*

[28]. *Oliveira et al.* [29] investigated the sensitivity of Fabry-Pérot cavities based on photopolymerizable adhesives for sensing application, which were sandwiched between the fibers and exhibited wavelength changes with temperature and humidity variations. *Leal-Junior et al.* [30] reported curvature sensors based on Fabry-Pérot cavities under two configurations: one used the adhesive between two single mode fibers and the other one with the adhesive between a single mode fiber and a perfluorinated POF.

On the other hand, FBGs with different polymer [31, 32] or metal [33,34] coatings can be used as chemical sensors, and by carefully choosing the coating material, they can be employed in harsh conditions [35], where the presence of oil, water or gaseous hydrocarbons needs to be monitored.

In this paper, extension of the work in [36], we report on a novel method for fabricating CFBGs in POF by post processing uniform gratings. An UV-curing optical adhesive is employed as coating in a portion of the grating (about half the grating length), and after initial coating tests a chirped POFBG device was obtained, showing good stability after its production. In addition, strain, humidity and temperature performance are characterized for potential sensing applications.

2. Bragg grating fabrication

The optical fiber employed was a 2-rings hexagonal hole microstructured PMMA fiber fabricated at *DTU Fotonik*, using the drill and draw method (fiber cross-section depicted in Fig. 1 (b)). It has an external average diameter of 138 μm and an average core diameter of 6.2 μm, with holes' diameter and pitch of 1.70 μm and 3.95 μm, respectively, resulting in a hole-pitch ratio of 0.43 which is less than the limit of 0.45, making it endlessly single mode [37]. Before the grating's inscription, the fiber was pre-annealed at 70 °C for 24 hours. A pulsed Q-switched Nd: YAG laser system (LOTIS TII LS-2137U Laser, emitting at the fourth harmonic (266 nm)) was used to perform the grating inscription (the inscription setup is shown in Fig.1(a)), using a repetition rate of 5 Hz and a pump energy of 24.6 J. A uniform phase mask, with a pitch of 567.8 nm, was used to fabricate an 8 mm long FBG, resulting in a central resonant Bragg wavelength in

the 850 nm region.

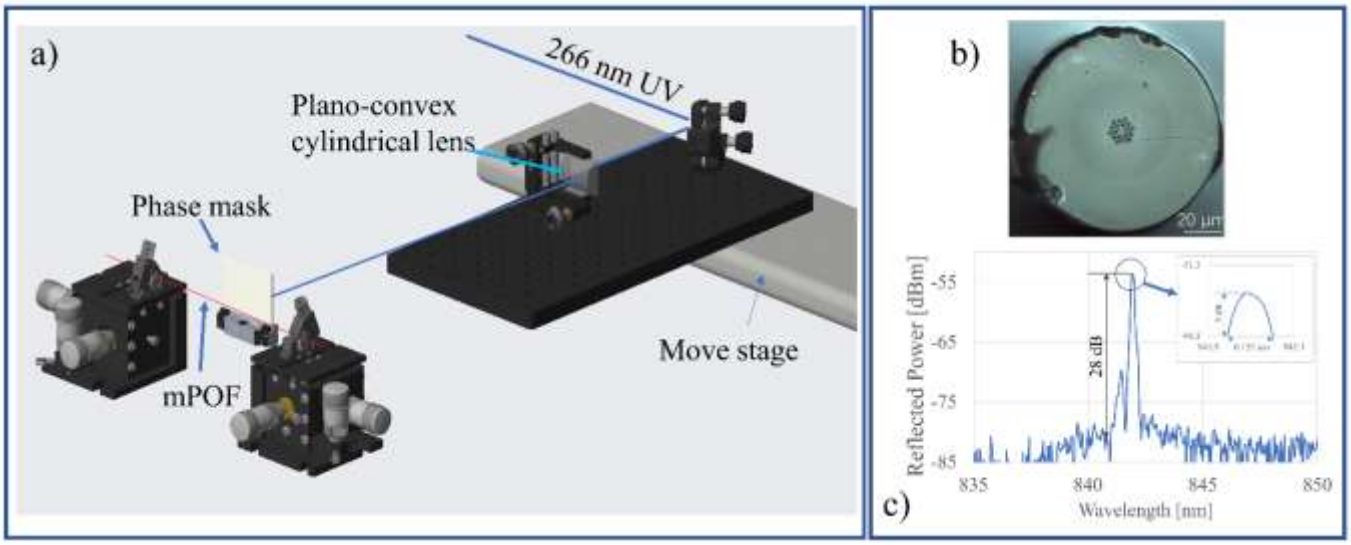

Fig. 1. a). Experimental setup for POFBG inscription; b) Cross-sectional view of the mPOF; c) Reflected spectrum of an 8 mm long uniform FBG inscribed in the mPOF (inset: 3 dB bandwidth).

A special room temperature cleaver was used to cleave the mPOF [38], and a commercial ceramic ferrule was applied for easy connectorization with an APC patch cord. The interrogation setup consisted of a super luminescent diode (Superlum SLD-371-HP1) launched into one of the arms of a 50:50 ratio single mode silica fiber optic coupler. The reflected spectrum was monitored with an YOKOGAMA optical spectrum analyzer (AQ6327). In Fig. 1 (c), the reflection spectrum of a uniform FBG inscribed with an exposure time of 3 minutes is depicted, presenting a resonant central wavelength around 841.9 nm, a 3-dB bandwidth of 155 pm and approximately 28 dB of reflected peak power.

3. Chirped Bragg grating production

After the POFBGs inscription, UV cure adhesives were applied on half of the grating length, with the initial purposes of obtaining different grating sections with distinct sensing capabilities and possibly producing a chirped grating during the process. Three different experiments were conducted here to achieve those goals and to improve the technology. In the first experiment, an adhesive (NOA 78, from Norland) coating was applied on half length of the grating (~4 mm) right after the POFBG inscription (see Fig. 2 (a)). Then, the adhesive was cured, for 30 seconds, by using a hand-held UV light source (Opticure LED 200 from Norland

Products Inc.) emitting at 365 nm wavelength and with a power density of 2.5 W/cm^2. The fiber was kept unstrained during the adhesive application and the UV curing process. Due to combination of polymerization effects and temperature increase during the UV curing process, the POFBG reflection spectrum suffered a small blue shift (~25 pm), as depicted in Fig. 2 (b).

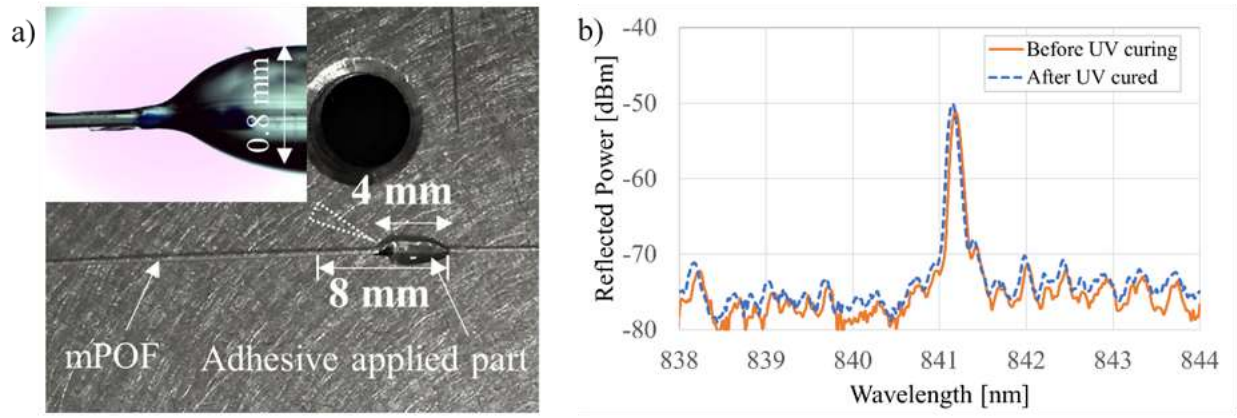

Fig. 2. a). The FBG inscribed in mPOF (8 mm long) with adhesive-based post-processing of half section of the grating. Inset: microscope image of a section of the coated POFBG; b). Reflection spectrum of the POFBG before and after the application of the adhesive coating.

It has been demonstrated that strain can assist in the chirped FBGs fabrication by employing a uniform phase mask [26], and increase the photosensitivity of undoped mPOFs [39]. Therefore, in the second experiment, the NOA 78 coating was applied again on half of the grating length while it was subjected to 8000 με. The grating reflection spectrum became broader after the UV light exposure, as depicted in Fig. 3, achieving a bandwidth of 11.7 nm, which consists in an increase of 700% compared with the uniform POFBG. It is important to note that since the chirped gratings presented here have an asymmetric reflection spectrum, for sensing purposes the Bragg wavelength can be set as the center between the recoded outer edges, defined as the first minima (yellow vertical lines in the graph of Fig. 3).

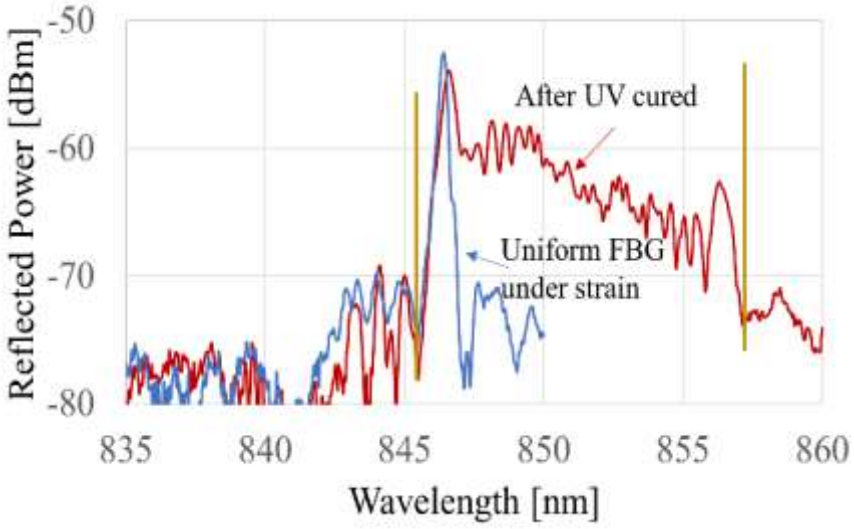

Fig. 3. Reflection spectrum of the grating before and after the application of the adhesive coating under 8000 με.

The chirp profile of the produced device is generated by the cure and consequently hardness and shrinkage of the UV adhesive coating, while the fiber is under strain, resulting in the presence of additional stress along the coated section. That stress is non-uniform and increases with the coating thickness. According to Fig. 2 (a) inset, there is a small section that makes the transition from the uncoated section of the grating to the coated section where the coating thickness becomes uniform along its length. In that small section, the coating thickness increases drastically from approximately 138 μm (fiber diameter) to approximately 1 mm due to the contact angle in the liquid adhesive when its applied on the optical fiber, resulting in different levels of stress in the fiber, which leads to the variation of the grating period (Λ) and consequently generates chirp in that area. The resulting POFBG device will then include 3 different grating sections as Fig. 4 demonstrates: the uncoated section, which presents a uniform grating (Uncoated FBG) with the same characteristics from inscription process; the coated section where the coating thickness is approximately uniform, which presents a uniform grating (Coated FBG) where $\Lambda_{\text{Coated FBG}} > \Lambda_{\text{Uncoated FBG}}$, and the small coated section (where the coating thickness varies) that stablishes the transition between Uncoated FBG and Coated FBG, and presents a chirped grating with a period variation from $\Lambda_{\text{Uncoated FBG}}$ to $\Lambda_{\text{Coated FBG}}$. Due to the hardening of the adhesive, fiber residual stress from the curing process will be in the coated section after the strain release, maintaining most of the chirped POFBG characteristics after the production

process. However, the grating device produced with NOA 78 coating was not stable after released, possibly due to the relative low modulus of elasticity (1140 psi), low hardness (55 of shore hardness) and high elasticity (approximately 57% elongation to failure) of the adhesive NOA 78 [40], whose characteristics are not suitable for the stability of the chirped grating device. Then, the use of other UV-curing optical adhesives with higher modulus of elasticity and hardness is a viable solution to improve the stability of the produced devices, specially after the strain release.

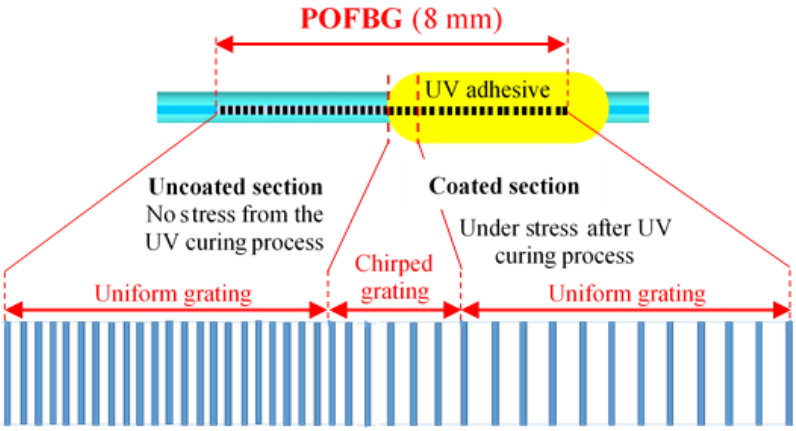

Fig. 4. Sketch of the produced chirped POFBG structure, with the respective period variation along the grating length, after the UV curing process.

Among the many optical adhesives available in the market, NOA 86 shows higher modulus of elasticity (360400 psi), higher tensile strength (7834 psi) and higher shore hardness (75) [40]. In the third experiment, NOA 86 coating was applied on half-length of an identical POFBG under 10000 με. As expected, from the previous experiment, the reflection spectrum became broader after UV exposure (with 5.8 nm bandwidth as Fig. 5 shows), which indicates that a clear stress performance appears after the UV exposure of the half-coated grating. In accordance with the previous results, the interface between the coated and uncoated sections of the grating shows some slope on the coating thickness, which implies a non-uniform stress performance that leads to the formation of a CFBG. Once the curing process was finished, the fiber was released and stabilized for 3 days. Fig. 5 shows the measured reflection spectrum, observing a bandwidth reduction down to 4.0 nm, which is narrower than the previous one but still showing a typical chirp performance.

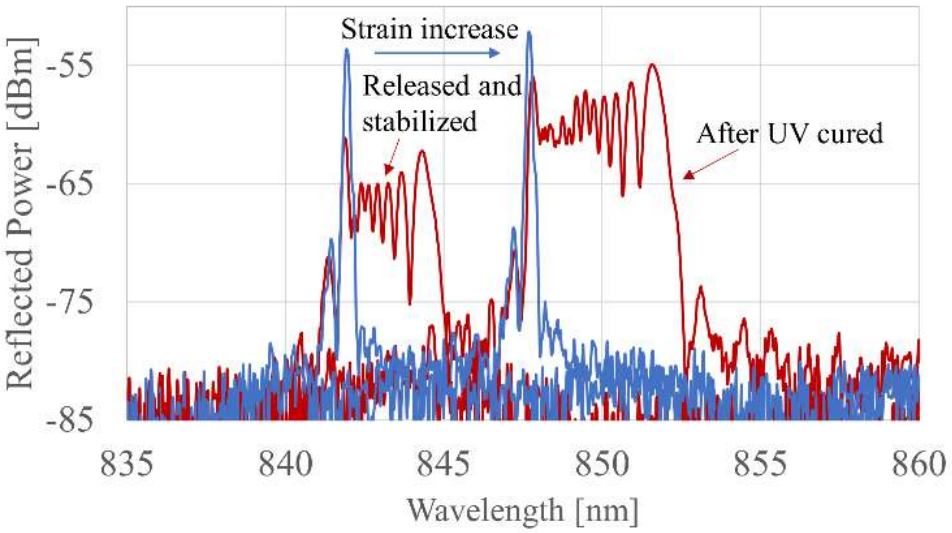

Fig. 5. Reflection spectra of the POFBG before and after applying the NOA 86, under 10000 με.

4. Strain, humidity and temperature performance

According to previous literature [41], the performance of the optical adhesive changes slowly with time, and therefore, post-annealing can be used to improve its stability. Therefore, the produced device was subjected to a post-annealing process where the grating was placed inside a climatic chamber (Angelantoni Industrie CH340) under 50 ºC for 12 hours without humidity control. The spectrum after post-annealing is shown in Fig. 6, where the bandwidth decreases to 1.5 nm, similar to the spectrum of the uniform POFBG [42]. During the post-annealing process, the adhesive coating lost part of its hardness causing the slipping of the fiber and the decrease/removal of the tensions generated during the curing process, which resulted in the loss of the chirp characteristics.

Nevertheless, after the post-annealing, and consequently after the loss the chirp profile, the resultant grating device was subjected to strain, humidity and temperature characterization to analyze the grating stability and sensing capabilities. In order to characterize the strain sensitivity, an 8.6 cm long fiber containing the grating was placed between two 3-axis stages (Thorlabs MBT616D). The fiber was strained above 8800 με with 800 με steps while awaiting 5 min between each step at room temperature (22 ºC). As shown in Fig. 6 (a) and Fig. 6 (b), the strain broadened the bandwidth of the reflection spectrum due to the half-coated

section of the grating, even after the post-annealing process. The performance of the coated and uncoated sections is different under strain application as Fig.6 (c) shows, since the reflection spectrum related to the uncoated section (peak 2) shifts with a sensitivity of 0.719±0.020 pm/με, but the reflection spectrum of the coated section (peak 1) shows a lower sensitivity of 0.122±0.005 pm/με, revealing its applicability for multiparameter sensing.

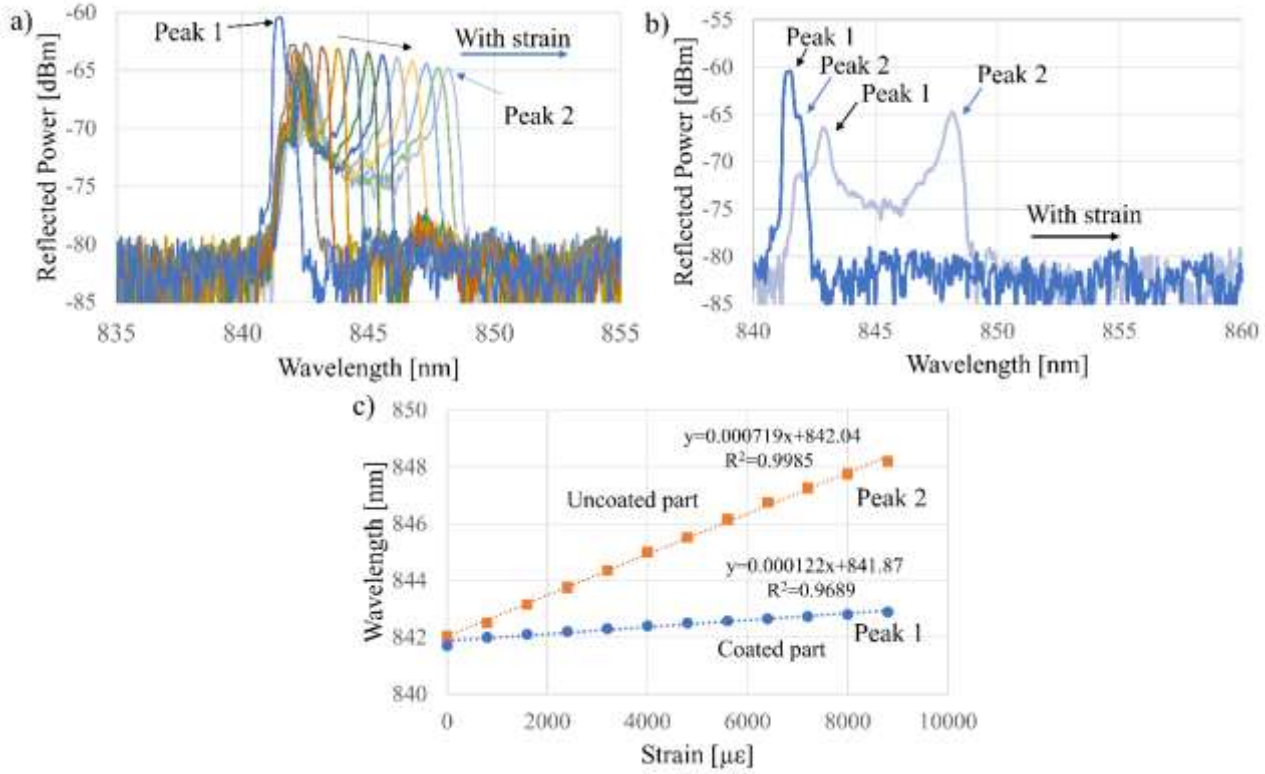

Fig. 6. a). The reflection spectrum shift for all the applied strain steps; b). Reflection spectrum of the grating with and without applied strain (0 and 8800 με, respectively); c). The Bragg wavelength shift with strain of two different peaks, which represent the coated and uncoated parts of the POFBG.

The obtained CFBG shows a different performance compared with the previous ones published in the literature, namely [26] and [27], where the bandwidth and the wavelength vary due to strain, as the period of the grating is non-uniform along its length. Here, as result of the production method and in part of the loss of the chirp characteristics during the post-annealing process, the obtained grating has shown a different strain response due to the coated and uncoated sections of the POFBG, which generates two distinct sensing sections (resulting in the appearance of two peaks), with a bandwidth of 7.80 nm under 8800 με, as Fig.6 shows.

In the following experiment, the same grating was subjected to 4000 με and placed inside the climatic chamber at 22 ºC in order to measure its humidity response. The relative humidity (RH) was increased from 30 % to 90 %, with 20 % steps (see Fig. 7(a)). The reflection spectra show that the left and right peaks have different behavior, since peak 1 shows a slightly lower sensitivity compared with peak 2. Fig. 7(b) indicates the sensitivity of each peak, achieving 11.8±0.2 pm /%RH and 13.7±0.5 pm/%RH for peak 1 and peak 2, respectively. This sensitivity difference confirms a different POFBG performance due to the optical adhesive coating applied on half section of the grating, where young's modulus increased after the curing process, reducing the swelling of the fiber in that region.

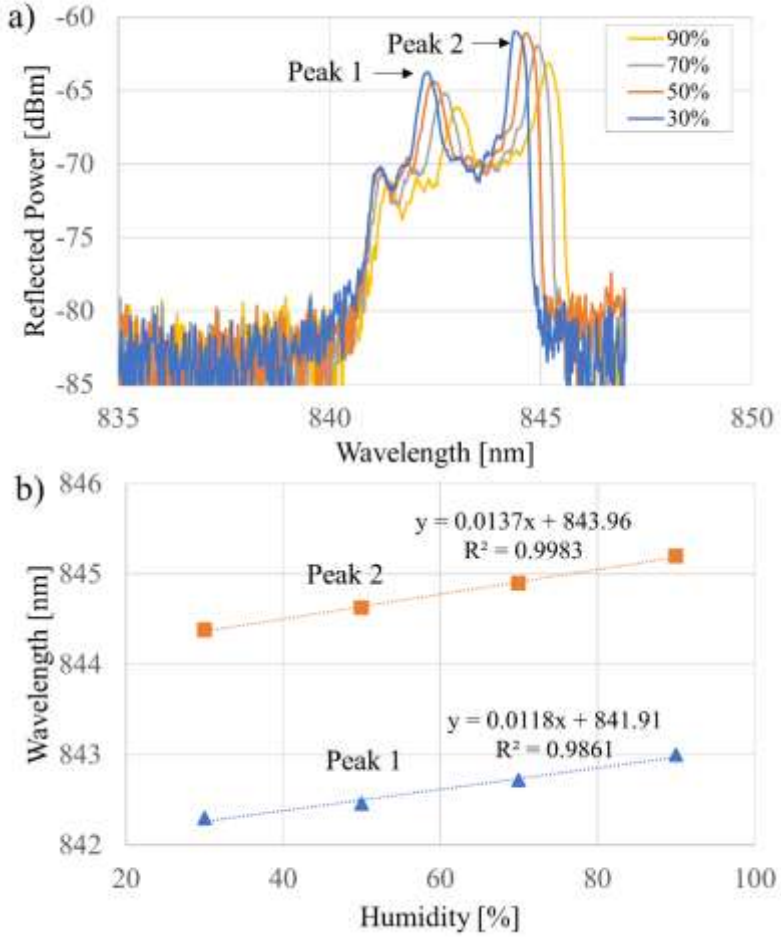

Fig. 7. a). Reflection spectra dependence on humidity. b). The Bragg wavelength shift of the two peaks with relative humidity changes.

The thermal characterization was conducted in the same climatic chamber under the identical strain conditions, while the humidity was set at 60 %. The temperature varied from 22 ºC to 37 ºC with 5 ºC steps (see Fig. 8 (a)), resulting in a linear shift of the peak 2 towards shorter wavelengths, showing linear performance with a sensitivity of -63.2±5.0 pm/ºC (see Fig. 8 (b)). Peak 1 shows a different performance

according to Fig. 8, due to the combination of the stress and viscosity changes imposed by the UV curing and temperature variations, respectively, resulting a blue shift followed by a red shift performance above 27 ºC at which point the fiber begins to slide in the coated section.

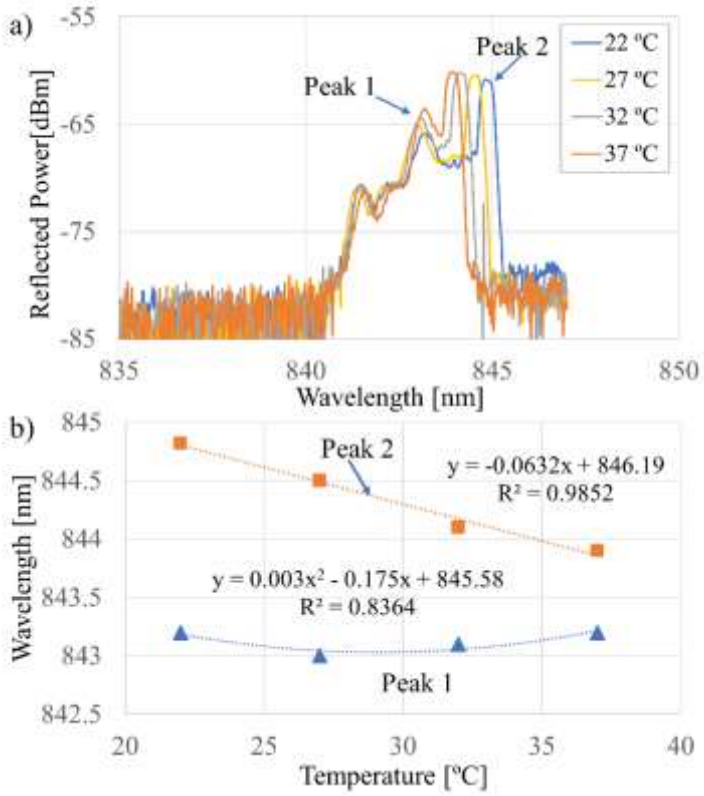

Fig.8. a). Reflection spectra dependence with increasing temperature. b). The Bragg wavelength shift of the two peaks with temperature changes.

5. Conclusion

To conclude, this paper presents a novel fabrication method for chirped Bragg gratings in polymer optical fibers. By using an UV-curing optical adhesive coating, we achieved chirped POFBGs, in which the bandwidth can be tunable when strain is applied. Gratings with two different segments were obtained for compact multiparameter sensing applications and their full characterization in terms of strain, humidity and temperature response was also studied. Different sensitivities were obtained for both strain and humidity characterization due to the presence of two distinct sensing active areas. For strain, the uncoated section shifts with a sensitivity of 0.719±0.020 pm/με, while the coated section shows a lower sensitivity of 0.122±0.005 pm/με. In the humidity test, the sensitivities of 11.8±0.2 pm /% and 13.7±0.5 pm/% were

achieved for the coated and uncoated sections, respectively. In the thermal characterization, due to the combination of the stress performance of UV curing and the viscosity change due to temperature variations, peak 1 (coated section) did not have a linear performance. These results show that this POFBG has some limitations when subjected to high temperatures, since the adhesive coating viscosity is also affected by this parameter. Nevertheless, this device could be employed in thermal sensing applications at lower temperatures, but further tests must be conducted to analyze the viability of this POFBG. The thermal limitations also affected the post-annealing process, in which more studies must be conducted in the future to optimize the process in order to avoid the loss of the chirp characteristics of the grating device and to obtain devices with relevant chirp for sensing applications. Also, comparing the sensing performance of the chirped grating devices with and without the post-annealing process might be interesting to investigate the importance of this thermal treatment in these devices. In addition, more studies must be conducted in the future to analyze the effects on the grating optical characteristics when the UV cure adhesive is applied on different length parts of the grating, including applied at different grating sections at the same time, the influence of different coating lengths and thicknesses and the performance of other UV cure adhesives. Also, obtaining linear slopes in the coating thickness, as well different slopes, is an interesting topic for future work to generate chirped gratings with a constant chirp. In summary, this fabrication method, which can be also employed with other optical fibers with considerable elastic coefficient, has high potential to develop chirped gratings with multiparameter sensing capabilities for different engineering applications, and possible biomedical applications through the combination of biocompatible POFs and UV cure adhesives.

Declaration of Competing Interest

The authors declare that they have no known competing financial interests or personal relationships that could have appeared to influence the work reported in this paper.

Acknowledgements

National Natural Science Foundation of China (62003046); The Spanish Ministerio de Ciencia, Innovación y Universidades RTI2018-101658-B-I00 FOCAL Project; Guangdong Basic and Applied Basic Research Foundation(2021A1515011997); Guangdong Recruitment Program of Foreign Experts (2020A1414010393); C. Marques acknowledges Fundação para a Ciência e a Tecnologia (FCT) through the CEECIND/00034/2018 (iFish project) and this work was developed within the scope of the project i3N, UIDB/50025/2020 &UIDP/50025/2020, financed by national funds through the FCT/MEC. Luis Pereira and Tiago Paixão also acknowledge FCT for the grant with references SFRH/BD/146295/2019 and PD/BD/128265/2016, respectively.

References

[1] A. Cusano, A. Cutolo and J. Albert, Fiber Bragg Grating Sensors: Recent Advancements, Industrial Applications and Market Exploitation, 1st ed. Sharjah, UAE: Bentham Science Publishers, 2011.

[2] D. J. Webb, Polymer fiber Bragg grating sensors and their applications in Optical Fiber Sensors Advanced Techniques and Applications, G. Rajan Ed. Boca Raton, FL, USA: CRC, 257–276 (2015).

[3] G. Emiliyanov, J.B. Jensen, P.E. Hoiby, L.H. Pedersen, E.M. Kjaer, L. Lindvold and O. Bang, (2007). Localized biosensing with Topas microstructured polymer optical fiber, Opt. Lett., 32(5), 460-462.

[4] J. Janting, J. Pedersen, G. Woyessa, K. Nielsen and O. Bang, (2019). Small and Robust All-Polymer Fiber Bragg Grating based pH Sensor. J. Lightwave Technol., 37(18), 4480-4486.

[5] J. Bonefacino, H. Y. Tam, T.S. Glen, X. Cheng, C. F. J. Pun, J. Wang, P. H. Lee, M.L.V. Tse and S.T. Boles, (2018). Ultra-fast polymer optical fibre Bragg grating inscription for medical devices. Light: Sci. & Appl., 7(3), 17161.

[6] Z. Xiong, G. D Peng, B Wu and P.L Chu, (1999). Highly tunable Bragg gratings in single-mode polymer optical fibers. IEEE Photon. Technol. Lett., 11(3), 352-354.

[7] G. Woyessa, A. Fasano, C. Markos, H.K. Rasmussen and O. Bang, (2017). Low loss polycarbonate polymer optical fiber for high temperature FBG humidity sensing, IEEE Photon. Technol. Lett., 29(7), 575-578.

[8] A. Fasano, G. Woyessa, P. Stajanca, C. Markos, A. Stefani, K. Nielsen, H. K. Rasmussen, K. Krebber and O. Bang, (2016). Fabrication and characterization of polycarbonate microstructured polymer optical fibers for high-temperature-resistant fiber Bragg grating strain sensors. Opt. Mater. Express, 6(2), 649-659.

[9] G. Woyessa, A. Fasano, C. Markos, A. Stefani, H. K. Rasmussen and O. Bang, (2017). Zeonex microstructured polymer optical fiber: fabrication friendly fibers for high temperature and humidity insensitive Bragg grating sensing. Opt. Mater. Express, 7(1), 286-295.

[10] G. Woyessa, H.K. Rasmussen and O. Bang, (2020). Zeonex - a route towards low loss humidity insensitive single-mode step-index polymer optical fibre. Opt. Fiber Tech., 57, 102231.

[11] W. Yuan, L. Khan, D.J.Webb, K. Kalli, H.K. Rasmussen, A. Stefani and O. Bang, (2011). Humidity insensitive TOPAS polymer fiber Bragg grating sensor. Opt. Express, 19(20), 19731-19739.

[12] C. Markos, A. Stefani, K. Nielsen, H.K. Rasmussen, W. Yuan and O. Bang, (2013). High-Tg TOPAS microstructured polymer optical fiber for fiber Bragg grating strain sensing at 110 degrees. Opt. Express, 21(4), 4758-4765.

[13] A. Lacraz, M. Polis, A. Theodosiou, C. Koutsides and K. Kalli, (2015). Femtosecond laser inscribed Bragg gratings in low loss CYTOP polymer optical fiber. IEEE Photon. Technol. Lett., 27(7), 693-696.

[14] R. Min, B. Ortega, A. Leal-Junior and C. Marques, (2018). Fabrication and Characterization of Bragg Grating in CYTOP POF at 600-nm Wavelength. IEEE Sensors Lett., 2(3).

[15] G. Woyessa, J. K. M. Pedersen, A. Fasano, K. Nielsen, C. Markos, H. K. Rasmussen and O. Bang, (2017). Zeonex-PMMA microstructured polymer optical FBGs for simultaneous humidity and temperature sensing. Opt. Letters, 42(6), 1161-1164.

[16] H. Dobb, D. J. Webb, K. Kalli, A. Argyros, M. C. J. Large and M. A. van Eijkelenborg, (2005). Continuous wave ultraviolet light-induced fiber Bragg gratings in few- and single-mode microstructured polymer optical fibers. Opt. Lett., 30(24), 3296–3298.

[17] L. Pereira, A. Pospori, P. Antunes, M.F. Domingues, S. Marques, O. Bang, D.J. Webb and C. Marques, (2017). Phase-Shifted Bragg Grating Inscription in PMMA Microstructured POF Using 248-nm UV Radiation. J. Lightwave Technol., 35(23), 5176-5184.

[18] X. Hu, C. F. J. Pun, H. Y. Tam, P. Mégret and C. Caucheteur, (2014). Tilted Bragg gratings in step-index polymer optical fiber. Opt. Letters, 39(24), 6835-6838.

[19] X. Hu, P. Mégret and C. Caucheteur, (2015). Surface plasmon excitation at near-infrared wavelengths in polymer optical fibers. Opt. Letters, 40(17), 3998-4001.

[20] R. Min, S. Korganbayev, C. Molardi, C. Broadway, X. Hu, C. Caucheteur, O. Bang, P. Antunes, D. Tosi, C. Marques and B. Ortega, (2018). Largely tunable dispersion chirped polymer FBG. Opt. Letters, 43(20), 5106-5109.

[21] S. Korganbayev, R. Min, M. Jelbuldina, X. Hu, C. Caucheteur, O.Bang, B. Ortega, C. Marques and D. Tosi , (2018). Thermal profile detection through high-sensitivity fiber optic chirped Bragg grating on microstructured PMMA fiber. J. Lightwave Technol., 36(20), 4723-4729.

[22] H.-Y. Chang, Y.-C. Chang, H.-J. Sheng, M.-Y. Fu, W.-F. Liu and R. Kashyap, (2016). An ultra-sensitive liquid-level indicator based on an etched chirped-fiber Bragg grating. IEEE Photonics Technol. Lett., 28(3), 268–271.

[23] H. Liu, H. Liu, G. Peng and T. W. Whitbread, (2005). Tunable dispersion using linearly chirped polymer optical fiber Bragg gratings with fixed center wavelength. IEEE Photon. Technol. Lett., 17(2), 411-413.

[24] C. A. F. Marques, P. Antunes, P. Mergo, D. J. Webb and P. André, (2017). Chirped Bragg gratings in PMMA step-index polymer optical fiber. IEEE Photon. Technol. Lett., 29(6), 500-503.

[25] A. Theodosiou, X. Hu, C. Caucheteur and K. Kalli, (2018). Bragg gratings and Fabry-Perot cavities in low-loss multimode CYTOP polymer fiber. IEEE Photon. Technol. Lett., 30(9), 857-860.

[26] R. Min, B. Ortega and C. Marques, (2018). Fabrication of tunable chirped mPOF Bragg gratings using a uniform phase mask. Opt. Express, 26(4), 4411-4420.

[27] R. Min, B. Ortega, C. Broadway, C. Caucheteur, G. Woyessa, O. Bang, P. Antunes and C. Marques, (2018). Hot water-assisted fabrication of chirped polymer optical fiber Bragg gratings. Opt. Express, 26(26), 34655-34664.

[28] X. Hu, C. F. J. Pun, H. Y. Tam, P. Mégret and C. Caucheteur, (2014). Highly reflective Bragg gratings in slightly etched step-index polymer optical fiber. Opt. Express, 22(15), 18807-18817.

[29] R. Oliveira, L. Bilro and R. Nogueira, (2018). Fabry-Pérot cavities based on photopolymerizable resins for sensing applications. Opt. Mater. Express, 8(8), 2208-2221.

[30] L. M.Avellar, C. A. Díaz, A. Frizera, C. Marques and M. J. Pontes, (2019). Fabry-Perot Curvature Sensor with Cavities based on UV-Curable Resins: Design, Analysis and Data Integration Approach. IEEE Sensors Journal, 19(21), 9798-9805.

[31] T.L. Yeo, T. Sun, K. T. V. Grattan, D. Parry, R. Lade and B.D. Powell, (2005). Characterization of a polymer-coated fiber Bragg grating sensor for relative humidity sensing. Sensors and Actuators B: Chemical, 110(1), 148-156.

[32] Á. G. Vila, M. Debliquy, D. Lahem, C. Zhang, P. Mégreta, C. Caucheteur, (2017). Molecularly imprinted electropolymerization on a metal-coated optical fiber for gas sensing applications. Sensors and Actuators B: Chemical, 244,1145-1151.

[33] S. Cai, Á. González-Vila, X. Zhang, T. Guo and C. Caucheteur, (2019). Palladium-coated plasmonic optical fiber gratings for hydrogen detection. Opt. Letters, 44(18), 4483-4486.

[34] X. Zhou, Y. Dai, J. M. Karanja, F. Liu, and M. Yang, (2017). Microstructured FBG hydrogen sensor based on Pt-loaded WO3. Opt. Express, 25(8), 8777-8786.

[35] X. D. Wang, and O.S. Wolfbeis, (2015). Fiber-optic chemical sensors and biosensors (2013–2015). Analytical chemistry, 88(1),203-227.

[36] R. Min, L. Pereira, T. Paixao, G. Woyessa, P. Andre, O. Bang, A. Frizera, P. Antunes, J. Pinto, Z. Li, B. Ortega and C. Marques, (2020). Adhesive assisted fabrication of chirped POF Bragg grating. Proceedings Volume 11355, Micro-Structured and Specialty Optical Fibres VI; 1135510.

[37] B. Kuhlmey, R. C. McPhedran and C. M. de Sterke, (2002). Modal cutoff in microstructured optical fibers. Opt. Lett., 27, 1684–1686.

[38] D. Sáez-Rodríguez, R. Min, B. Ortega, K. Nielsen and D.J Webb, (2016). Passive and portable polymer optical fiber cleaver. IEEE Photon. Technol. Lett., 28(24), 2834-2837.

[39] D. Sáez-Rodríguez, K. Nielsen, O. Bang and D. J. Webb, (2014). Photosensitivity mechanism of undoped poly (methyl methacrylate) under UV radiation at 325 nm and its spatial resolution limit. Opt. Letters, 39(12), 3421-3424.

[40] Norland Adhesive Selector Guide: https://www.norlandprod.com/adhchart.html (access 14/12/2020)

[41] F. Zhang, X. Xu, J. He, B. Du and Y. Wang, (2019). Highly sensitive temperature sensor based on a polymer-infiltrated Mach–Zehnder interferometer created in graded index fiber. Opt. Letters, 44(10), 2466-2469.

[42] R. Min, L. Pereira, T. Paixao, G. Woyessa, P. Andre, O. Bang, P. Antunes, J. Pinto, Z. Li, B. Ortega and C.Marques,(2019). Inscription of Bragg gratings in undoped PMMA mPOF with Nd:YAG laser at 266 nm wavelength, Opt. Express, 27(26), 38039-38048.